



UvA-DARE (Digital Academic Repository)

Improving superficial hyperthermia treatment

Temperature matters

Bakker, A.

Publication date

2021

[Link to publication](#)

Citation for published version (APA):

Bakker, A. (2021). *Improving superficial hyperthermia treatment: Temperature matters*. [Thesis, fully internal, Universiteit van Amsterdam].

General rights

It is not permitted to download or to forward/distribute the text or part of it without the consent of the author(s) and/or copyright holder(s), other than for strictly personal, individual use, unless the work is under an open content license (like Creative Commons).

Disclaimer/Complaints regulations

If you believe that digital publication of certain material infringes any of your rights or (privacy) interests, please let the Library know, stating your reasons. In case of a legitimate complaint, the Library will make the material inaccessible and/or remove it from the website. Please Ask the Library: <https://uba.uva.nl/en/contact>, or a letter to: Library of the University of Amsterdam, Secretariat, P.O. Box 19185, 1000 GD Amsterdam, The Netherlands. You will be contacted as soon as possible.

CHAPTER 6

TWO HIGH-RESOLUTION THERMAL MONITORING SHEETS FOR CLINICAL SUPERFICIAL HYPERTHERMIA

Akke Bakker
Remko Zweije
Geertjan van Tienhoven
H. Petra Kok
Jan Sijbrands
H.J.G. Desirée van den Bongard
Coen R.N. Rasch
Hans Crezee

Published in Physics in Medicine & Biology 2020; 65(17) 175021, doi: 10.1088/1361-6560/ab9bc2

ABSTRACT

Background: Temperature measurement during superficial hyperthermia is limited by poor spatial resolution. We investigated two sheets to improve temperature monitoring of the skin surface.

Materials and Methods: Two different sheets were studied with a grid of temperature sensors with one sensor per $\sim 5 \text{ cm}^2$. The first was a matrix of multisensor thermocouple probes laced through a silicone sheet. The second sheet had rows of thermistors connected by meandering copper leads mounted on stretchable printed circuit board (SPCB). Accuracy, temperature resolution and two hour stability of both sheets were investigated. Furthermore, we determined the ability to follow body contours, thermal conduction errors and electromagnetic (EM) compatibility to clinically used 434 and 915 MHz hyperthermia applicators.

Results: For both sheets the accuracy ($\leq 0.2 \text{ }^\circ\text{C}$), temperature resolution ($\leq 0.03 \text{ }^\circ\text{C}$) and stability ($\leq 0.01 \text{ }^\circ\text{C h}^{-1}$) were adequate for clinical use. Thermal conduction errors ranged from 5.25 - 11.25 mm vs. 2.15 mm for the thermocouple probe and thermistor, respectively. Both sheets could follow body contours, where the ratio air/ water bolus surface was $< 5 \%$. When aligned perpendicularly to the EM field the meandering copper tracks used on the SPCB did induce self-heating, while the thermocouple probes did not. Self-heating had a linear relationship with the angle of the leads with respect to the EM field direction for both sensors at both frequencies. Self-heating of the thermistor was similar for both frequencies, while it was approximately two-fold higher for 915 vs. 434 MHz for the thermocouple.

Conclusion: The use of SPCB technology for skin surface monitoring was promising. However, suppressing self-heating induced by the horseshoe shaped copper tracks needed for stretchability of the SPCB requires more in-depth investigation. The thermocouple matrix was the most promising for clinical application, meeting 6/7 of the major requirements for skin surface temperature monitoring when positioned perpendicular to the EM field.

INTRODUCTION

Hyperthermia, raising tissue temperature to 40 - 44 °C, is a known radio- and chemosensitizer. Dose effect relationships have been found in both retrospective and prospective studies for a wide range of temperature and thermal dose variables [1-10]. Sufficiently high temperatures are necessary to achieve the sensitizing effect, while local hotspots can cause thermal toxicity such as blisters and fat necrosis [1, 10-16]. Adequate thermometry feedback is thus essential to ensure high quality treatments.

Electromagnetic (EM) radiative hyperthermia is the most frequently applied technology to heat superficial disease up to 2 - 3 cm (915 MHz, USA) and up to 3 - 4 cm deep (434 MHz, Europe). Monitoring the temperature in an EM field is associated with challenges, especially since an accuracy of ± 0.2 °C is required. [17] When metal sensors are placed inside an EM field interactions with the electronics can occur, thermal conduction errors can be induced and the probe can show self-heating [18]. Present clinically accepted thermometry methods have resolved these issues [18, 19]. Unlike regular thermistors, thermistors with high-resistance leads (e.g. Bowman probes) can be used safely and accurately (accuracy within 0.1 °C) in an EM field without restrictions. Under several conditions thermocouples and thermistors with metal leads can also measure the temperature within 0.1 °C. The probes should be positioned perpendicular to the direction of the EM field, if possible, and the power must be switched off for several seconds before the temperature read out [18]. For multisensor thermocouple probes consisting of metal wires, thermal smearing along the probe can influence the accuracy of temperature measurements [20], particularly in regions with high temperature gradients. Fiber-optic probes can be used without any problems in an EM field. However, they are high in costs and fragile. Non-invasive thermometry methods such as radiometry, magnetic resonance-, infrared-, and ultrasound thermometry are not feasible because, among others, a coupling water bolus is placed between the applicator and the skin surface.

Present clinical techniques for monitoring skin surface temperature distributions during superficial hyperthermia treatments generally consist of mounting a number of single sensor or multisensor probes at various locations on skin and scar tissue [21]. A recent numerical simulation study found that at least 50 sensors per 400 cm² applicator are needed to adequately measure the surface temperature distribution (1 sensor per 8 cm²). Moreover, to adequately monitor hotspots more than 100 stationary sensors were advised (1 sensor per 4 cm²). [22] Unfortunately, commercial microwave hyperthermia systems generally offer only eight single sensors (ALBA ON 4000, Medlogix, Italy; BSD-500, Pyrexar, Salt Lake City, UT, USA). As a result, temperature in most of the skin surface remains unmonitored.

Several academic groups have investigated solutions to improve the spatial resolution of thermal monitoring during superficial microwave hyperthermia. The most used solution is an individualized grid of stationary temperature measurement points distributed over the target area. Presently, the Erasmus MC (Rotterdam, the Netherlands) applies eight four sensor fiber-optic probes with 20 mm spacing (THR-NS-1164C, FISO Technologies Inc., Quebec, Canada) connected to a 32 channel thermometry system [23]. In our center, the Amsterdam UMC (Amsterdam, the Netherlands), multisensor copper-constantan thermocouple probes (ELLA-CS, Hradec Králové, Czech Republic) with seven or fourteen sensors per probe are utilized [22]. The thermometry system (UMCU, Utrecht, the Netherlands) can read out 196 sensors (28 seven sensor probes) in 0.32 seconds [24]. In 2008 the group at Duke University developed a conformal thermal monitoring sheet to measure the surface temperature distributions during superficial hyperthermia treatment. It comprises of a multilayer Kapton film with multiple plastic catheters which contain 16 single fiber optic sensors (IPITEK, Carlsbad, California, US) arranged in a 40 x 40 mm grid. [21, 25] Although these methods substantially improve the spatial resolution of thermal monitoring, they are either too expensive, time-consuming, or require experienced users, thereby limiting clinical implementation in hyperthermia centers worldwide.

In this paper, two potential sheets for improved skin surface temperature monitoring during superficial hyperthermia are introduced. Both employ temperature probes which should be readily adoptable by the suppliers of currently available hyperthermia devices. The accuracy, temperature resolution, stability and thermal conduction errors of both methods are investigated. The flexibility of the supporting material is investigated, as well as the EM compatibility.

MATERIALS

The major requirements of a sheet to perform skin surface temperature monitoring during superficial hyperthermia are:

- Spatial resolution of 40 x 40 mm; preferably 20 x 20 mm [22]
- Accuracy ≤ 0.2 °C [17]
- Temperature resolution ≤ 0.1 °C [17]
- Stability ≤ 0.1 °C h⁻¹
- Thermal conduction errors ≤ 10 mm
- Body conformal
- Electromagnetically compatible

Two potential sheet designs to improve skin surface temperature monitoring during superficial hyperthermia were investigated. The first sheet was developed in collaboration with Medlogix (Rome, Italy) to ensure fast, precise and reproducible sensor placement during superficial hyperthermia treatment and to allow an accurate reconstruction of the skin surface temperature. It consists of a rigid supportive structure, attached to a thermocouple matrix consisting of a 0.3 mm thick flexible silicone sheet with eight multisensor thermocouple probes (ELLA-CS, Hradec Králové, Czech Republic) laced through the sheet every 20 mm. The thermocouple matrix contains 56 sensors (Figure 1), with a spatial resolution of 20 x 25 mm (Table 1). The probes consist of one common constantan wire (\varnothing 70 μ m) and seven copper wires (\varnothing 40 μ m), welded at 25 mm intervals. The thermocouple probe was surrounded by a Teflon coating (\varnothing 0.5 mm) and the end of the tube was sealed with epoxy. The thermocouple probes can be secured to keep the sensors in a fixed position. The probes were laced through the silicone sheet, such that all sensors were positioned beneath the silicone sheet, resulting in a directional sensitivity of the sensor towards the skin surface. The thermocouple matrix has a minimum thickness of 0.3 mm, at the position of the thermocouple probes the thickness is maximal, e.g. 0.8 mm. A multi-channel thermometry system was required for temperature read-outs, e.g. the 196 channel Utrecht thermometry system (UMCU, Utrecht, the Netherlands) [24] or the commercially available 64 channel ALBA thermometry system with a temperature resolution of 0.0156 °C (Medlogix, Rome, Italy).

Table 1. Characteristics of the two high-resolution thermal monitoring sheets that were developed to improve the skin surface temperature monitoring during superficial hyperthermia.

| | Matrix | | SPCB | |
|----------------------------|---|----------------------------|--|------------------------|
| Sensor | | | | |
| Type | Thermocouple | | 100 k Ω NCT thermistor (0805 SMD) | |
| Material | Copper-constantan | | NiSn terminations, glass coated | |
| Size | ~0.5 mm (length weld) | | 0.9 x 1.3 x 2.15 mm (H x W x L) | |
| Sensors per probe | 7 | | | |
| Spacing | 25 mm | | | |
| Manufacturer | ELLA-CS, Hradec Králové, Czech Republic | | Vishay Intertechnology, Malvern, Pennsylvania, USA | |
| Thermal response time | 1.5 s [24] | | 10 s [28] | |
| Connecting tracks | | | | |
| Material | <i>Copper</i> | <i>Constantan</i> | <i>Copper</i> | |
| Wires/ probe | 7 | 1 | | |
| Size | \varnothing 0.04 mm | \varnothing 0.07 μ m | 0.015 x 0.1 mm (H x W) | |
| Mean distance tracks | | | 3.33 mm | |
| Minimum length | 25 mm | | 25 mm | |
| Maximum length | 187.5 mm | | 125 mm | |
| Shape | Straight | | Horseshoe shaped meanders | |
| Supporting material | | | | |
| Type | <i>Sheet</i> | <i>Coating</i> | <i>Sheet</i> | <i>SMD cover layer</i> |
| Material | Silicone | Teflon | Polyurethane | Epoxy |
| Height | 0.3 mm | | 0.1 mm | ~0.025 mm |
| Size (width x length) | 166 x 212.5 mm | | 150 x 150 mm | ~size SMD + 0.05 mm |
| OD | | 0.5 mm | | |
| Sheet | | | | |
| Dimensions | 166 x 212.5 mm | | 150 x 150 mm | |
| Minimum thickness | 0.3 mm | | 0.1 mm | |
| Maximal thickness | 0.8 mm (\varnothing 0.5 mm probe + 0.3 mm sheet) | | 1.0 mm (0.9 mm sensor + 0.1 mm sheet) | |
| Spatial resolution | 25 x 20 mm | | 20 x 20 mm | |
| Sensors | 56 | | 25 - 100 (combination 1 - 4 sheets) | |

Abbreviations: SPCB= stretchable printed circuit board, NTC= negative temperature coefficient, SMD= surface mounted device, H= height, W=width, L= length, ID= inner diameter, OD= outer diameter.

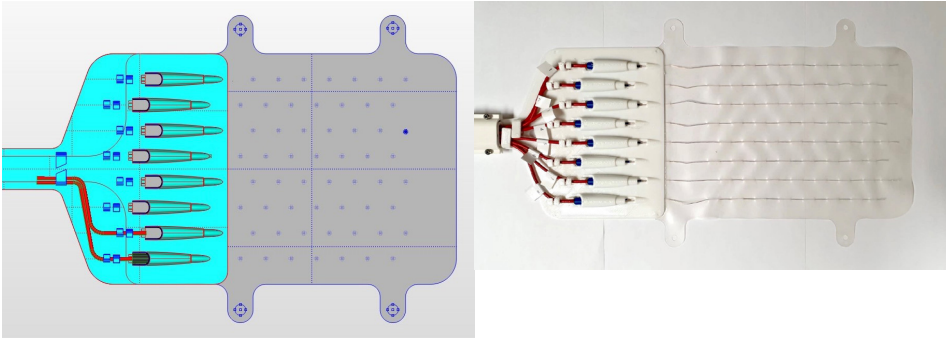


Figure 1. The prototype of the thermocouple matrix (Medlogix, Rome, Italy). Dimensions of the silicone sheet were 0.3 - 0.8 x 166 x 212.5 mm. The sheet had a 20 x 25 mm grid of 56 sensors.

The second sheet consists of a stretchable printed circuit board (SPCB) with a 20 x 20 mm grid of thermistors (QPI group, Helmond, the Netherlands) (Figure 2). It is a modular system, where multiple sheets can be combined, resulting in 25 - 100 sensors (Table 1). Stretchability and flexibility were obtained by shaping the copper tracks (width 100 μm , height 15 μm) as horseshoe shaped meanders. As a basis two 50 μm polyurethane sheets were used to embed the tracks and the components thus serving as a circuit carrier [26, 27]. At the positions of the thermistors, a laser cuts out the top polyurethane layer and multiple 100 k Ω surface mounted device (SMD) negative temperature coefficient (NTC) thermistors (NTCS0805E3104*MT, Vishay Intertechnology, Malvern, Pennsylvania) were soldered on the copper pads using low melting temperature solder SnBi (melting temperature 138 $^{\circ}\text{C}$; CR11, EDSYN, London, United Kingdom). Afterwards a layer of epoxy was used to seal off the thermistor from air. [27] In general, the SPCB is 0.1 mm thick, at the position of the thermistor the sheet is 1.0 mm thick.

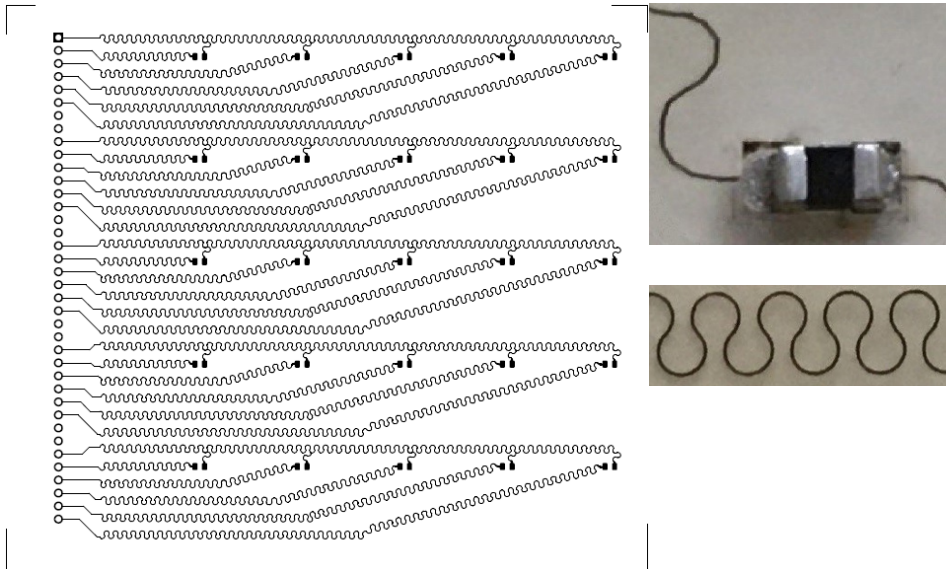


Figure 2. The design of the electrical circuit of the stretchable printed circuit board and magnified sections of the sheet (QPI group, Helmond, the Netherlands). The sheet had a 20 x 20 mm grid of 25 thermistors, the dimensions were 0.1 - 1.0 x 150 x 150 mm.

METHODS

Both sheets consist of multiple sensors, connecting tracks and supporting material. The accuracy, temperature resolution and stability of the electrical circuit were analyzed and its thermal conduction errors were investigated. Furthermore, we analyzed whether the supporting material was sufficiently stretchable and flexible to follow patient body contours. Finally, we investigated whether there was perturbation of the temperature readings due to microwave interference with the electrical circuits.

Electrical circuit

Accuracy

The accuracy of a seven sensor copper-constantan thermocouple probe (ELLA-CS, Hradec Králové, Czech Republic) and a 100 k Ω NTC thermistor (NTCS0805E3104*MT, Vishay Intertechnology, Malvern, Pennsylvania, USA) were determined based on intercomparison to a calibrated resistive temperature device; the Pt100 (temperature resolution 0.001 $^{\circ}\text{C}$, accuracy ≤ 0.02 $^{\circ}\text{C}$; Model 935-14-61, Isotech, Southport, UK). The intercomparisons were performed over a 25 - 50 $^{\circ}\text{C}$ temperature range in a temperature controlled circulating water bath (LAUDA-Brinkmann, Delran, NJ, USA). After achieving stable temperature, the maximum temperature fluctuation of the water bath never exceeded 0.04 $^{\circ}\text{C}$. The acceptable accuracy was ± 0.2 $^{\circ}\text{C}$ [17]. The thermocouple was calibrated between 25 and 45 $^{\circ}\text{C}$ and read out via the Utrecht thermometry system (UMCU, Utrecht, the Netherlands), which was in clinical use at our institute. The thermistor was read out via a digital multimeter (GW Instek, GDM-8341, Taipei, Taiwan), the measured resistance was transformed to temperature using the online available curve-computation list for the SMD0805 thermistor [28]. The Pt100 connects directly to the computer. A software program was developed to read out all three probes simultaneously with sample frequency 1 Hz for the thermocouple and Pt100, and 0.5 Hz for the thermistor (java, version 1.8). For each temperature increment, after achieving a stable temperature, the accuracy and its standard deviation during 60 seconds were reported.

Temperature resolution

The temperature resolution of the SPCB was calculated for the scenario when the SPCB was connected to a 10 bits (b) analog digital converter and the temperature range of interest 20 - 50 $^{\circ}\text{C}$. The temperature difference (ΔT) can be divided by 2^b to determine the temperature resolution.

$$\text{Resolution } (^{\circ}\text{C}) = \frac{\Delta T}{2^b}$$

Stability

The clinically relevant stability was determined as the variation of thermometer response over the clinical treatment time of up to 2 hours in a fixed temperature water bath at 42 °C (LAUDA-Brinkmann, Delran, NJ, USA). A maximum change of 0.1 °C h⁻¹ was considered acceptable in this time period.

Thermal conduction errors

In sensors with metal leads such as thermocouples and thermistors, thermal conduction along the leads causes axial smearing [20, 29]. We experimentally investigated the thermal conduction errors of both sensors. A thermal conduction error of 10 mm along the leads was considered acceptable, since the spacing of the sensors on the thermocouple probe was 25 mm.

To establish the conduction error a set up with compartments at different temperatures was used in which a temperature step of approximately 10 °C was applied to both a seven sensor copper-constantan thermocouple probe with 20 mm spacing and one 100 kΩ thermistor. For this experiment the thermistor was soldered to two 25 μm copper leads, where one lead was U-shaped (length U-shape 75 mm; Figure 3c). The sensors were pulled through a small hole in a 50 μm membrane (40 x 40 mm) from a cold insulated inner region (cube of 20 x 20 x 20 cm) to a warm outer region (Figure 3). The water temperatures were kept constant using three heaters with a pump function (LAUDA-Brinkmann, Delran, NJ, USA) and one cooler (ETK50, LAUDA-Brinkmann, Delran, NJ, USA). The step response was measured by moving the sensors automatically with an in-house built positioning system (resolution 0.1 mm; XYZ robot assembled from parts from Igus, Cologne, Germany) in 0.5 mm steps over a distance of 150 mm. Each sensor will cross the division, enabling us to study smear as a function of the number of tracks. The step response function was quantified by determining the width of the 10 % to 90 % temperature step [20].

Body conformity

The conformity to body contours of each sheet was investigated in three patients, with locoregional recurrent breast cancer, who all signed an informed consent (IRB AUMC: XT4-148). In our center, a standard CT-scan was made to verify the position of the additional invasive catheter that was placed for temperature measurements during hyperthermia treatment. During the CT-scan, the sheets were positioned on the contralateral chest wall with a 180 x 200 mm water bolus (part from the Beta applicator; Medlogix, Rome, Italy) on top. The amount of air between the water bolus (17 x 28 cm) and the skin of the patient was delineated in Velocity version 4.0 (Varian, Crawley, UK) for all six patients. The surface area of air with respect to the surface area of the water bolus was analyzed. Air bubbles between the water bolus and skin surface

may influence the specific absorbed ratio (SAR) distribution pattern of the applicator. Therefore we set a conservative limit of 1 % for an individual air bubble and 5 % for all air with respect to the surface area of the water bolus.

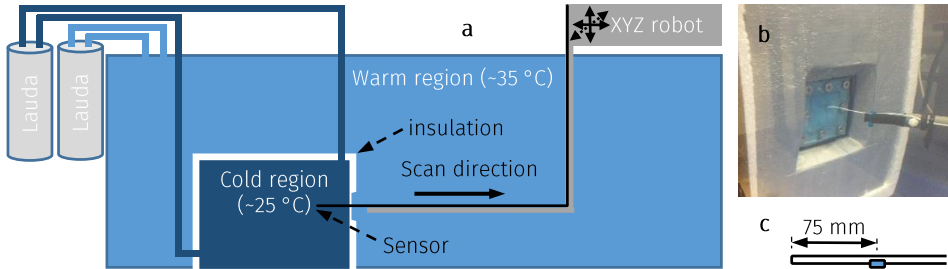


Figure 3. (a) The experimental set-up to measure thermal conduction errors of the thermocouple probe and the thermistor. The sensors were mechanically pulled with a XYZ robot from a cold insulated region (approximately 25 °C) to a warm region (approximately 35 °C). (b) Photograph of the thermistor that passes the 50 µm membrane. (c) To pass the membrane, one copper lead of the thermistor was U-shaped.

Electromagnetic compatibility

The electromagnetic compatibility (EMC) of both sheets in 434 and 915 MHz EM fields was investigated. The EM fields were generated with either a gamma applicator (Medlogix, Rome, Italy) [30, 31] connected to a 434 MHz ALBA Double ON-4000 system (Medlogix, Rome, Italy) or with a MA-100 applicator (Pyrexar Medical, Salt Lake City, USA) [32–34] connected to a 915 MHz generator (Elrad S.a.s., Milan, Italy). The influence of the angle of the tracks (0 - 90 °) with respect to the main direction of the EM field was investigated, while the sensors were positioned at the center of the applicators. For the first EMC experiment, a 100 kΩ NTC thermistor was soldered to two standard 25 µm copper leads. Both the thermistor and the thermocouple were placed centrally between two water boluses circulating at 40 °C (Figure 4). A muscle-equivalent phantom was placed beneath the second bolus. After achieving a stable water temperature of 40 °C at both water bolus inlets, power was turned on for three minutes at 50 W. Afterwards the temperature decay was measured for three minutes. The sample frequency of the thermocouple probe was 1 Hz vs. 0.5 Hz for the thermistor. The amount of self-heating of the sensor was quantified by the temperature decay at time τ , where τ was the thermal time constant (i.e. 63.2 % of the final value) of the temperature decay after turning the power off. Every measurement was repeated at least twice. Different time-dependent behavior may be expected for thermocouples and thermistors due to differences in size and mass. The thermal time constant (τ) and the temperature decay at time τ were reported, the last being an indication of self-heating. A maximum thermal time constant of five seconds was acceptable, while self-heating was considered acceptable when ≤ 0.1 °C.

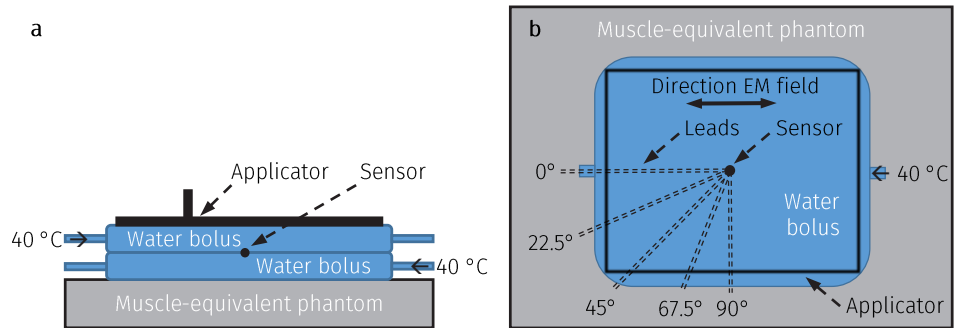


Figure 4. The experimental set-up to test the electromagnetic (EM) compatibility of a thermocouple and a thermistor to 434 and 915 MHz; (a) side view, (b) top view. The sensor was positioned between two water boluses circulating at 40 °C, with a muscle-equivalent phantom below.

For the SPCB, the influence of the horseshoe shaped meandering copper tracks was investigated in the same experimental set-up, where the traces were positioned perpendicular to the main direction of the EM field (Figure 2). The distance of the horseshoe shaped copper meandering tracks positioned inside the EM field was varied from 25 - 105 mm.

RESULTS

Electrical circuit

Accuracy

The accuracy in the temperature range from 25 to 50 °C was 0.06 ± 0.07 °C versus 0.03 ± 0.02 °C for the thermocouple and the thermistor, respectively (Figure 5, Table 2). At temperatures outside the calibration range (> 45 °C) the thermocouple was less accurate, with a maximum deviation of -0.18 °C at 50 °C. The maximum deviation of the thermistor was -0.05 °C at 28 °C. Both sheets satisfied the ± 0.2 °C accuracy criterion [17] at all temperature levels between 25 - 50 °C.

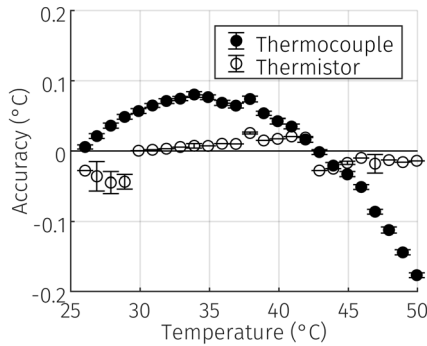


Figure 5. The mean accuracy \pm standard deviation in the temperature range 25 to 50 °C of the first sensor of a multisensor copper-constantan thermocouple probe (ELLA-CS, Hradec Králové, Czech Republic) and one 100 k Ω negative temperature coefficient thermistor (NTCS0805E3104*MT, Vishay Intertechnology, Malvern, Pennsylvania).

Temperature resolution

When the 10 bits ADC was limited from 20 to 50 °C for temperature measurement, the temperature resolution of the thermistor was 0.0293 °C (Table 2). The SPCB satisfied the temperature resolution criterion of 0.1 °C [17].

Stability

Both the thermocouple probe and the thermistor remained stable for the duration of a hyperthermia treatment (Figure 6). The deviation was less than 0.01 °C h⁻¹ for both the copper-constantan thermocouple probe and the 100 k Ω NTC thermistor, respectively (Table 2).

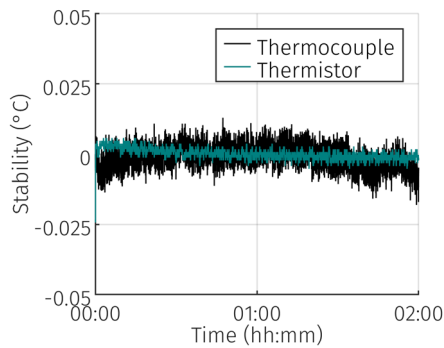


Figure 6. The two hour stability of the first sensor of a multisensory copper-constantan thermocouple probe (ELLA-CS, Hradec Králové, Czech Republic), and one 100 k Ω negative temperature coefficient thermistor (NTCS0805E3104*MT, Vishay Intertechnology, Malvern, Pennsylvania).

Thermal conduction errors

Temperature data measured by the seven sensors of the thermocouple probe and one thermistor crossing the division between two water baths at approximately 25 °C and approximately 35 °C were shown in Figure 7. The thermocouple probe shows more axial smearing than the thermistor. The width of the 10 % to 90 % temperature step was 8.74 ± 2.18 mm (mean \pm SD) for the thermocouple probe versus 2.15 mm for the thermistor, respectively (Table 2). The axial smearing increases with the number of wires inside the thermocouple probe, where sensor A in the tip had less smearing than the last sensor G, 5.25 vs. 11.25 mm, respectively.

Body conformity

Each sheet could follow the body contours of three patients (Figure 8, Table 3). Small air bubbles could be noticed between the matrix or SPCB and the patients. These air bubbles were often located in the close vicinity of the thermocouple probes and thermistors. Air bubbles had an average thickness of 0.2 cm. The air surface with respect to the water bolus surface was 4.6 ± 0.5 % ($n = 3$) and 2.8 ± 0.6 % ($n = 3$) for the matrix and SPCB, respectively (Table 2). The largest air bubble comprised 0.9 % of the surface area of the applicator (Table 3).

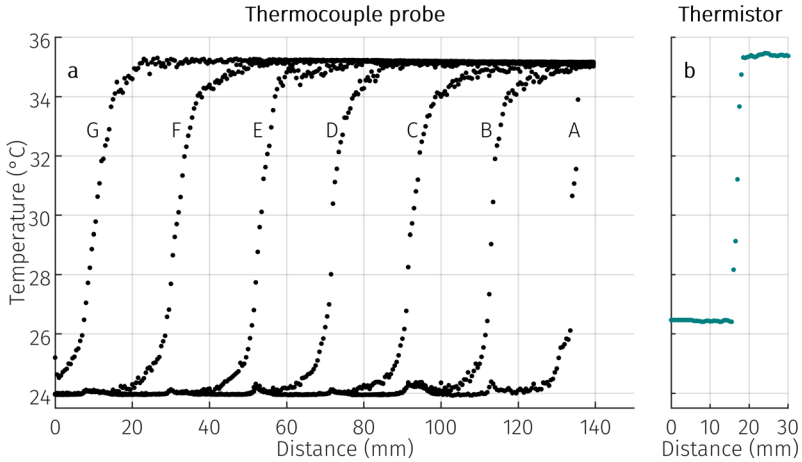


Figure 7. Step response of (a) a copper-constantan thermocouple probe (ELLA-CS, Hradec Králové, Czech Republic) and (b) a 100 k Ω negative temperature coefficient thermistor (NTCS0805E3104*MT, Vishay Intertechnology, Malvern, Pennsylvania). The thermocouple probe had seven sensors where the sensor in the tip was A, and the final sensor was G.

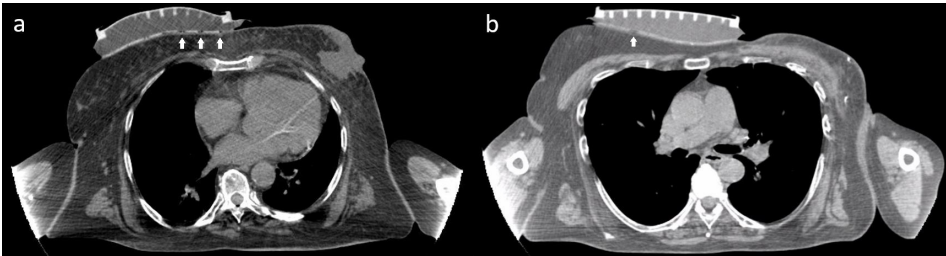


Figure 8. CT-scans show the conformity of (a) the thermocouple matrix and (b) the stretchable printed circuit board (SPCB) to the bodies of two different patients with locoregional recurrent breast cancer. The white arrows indicate the location of small air bubbles.

Electromagnetic compatibility

The EMC was quantified for the first sensor of the thermocouple probe and the thermistor. At 434 MHz no self-heating was observed when the straight leads were positioned perpendicular to the EM fields (90°; Figure 9a, c). The angles of the leads to the EM field showed a linear relationship with self-heating, which was represented by the temperature decay at time τ . Both sensors showed self-heating when the leads were not positioned perpendicular to the EM fields. With thermal time constants of 3.2 ± 0.8 s vs. 6.4 ± 0.9 s for the thermocouple vs. the thermistor in a 434 MHz EM field (Table 2). In a 915 MHz EM field the thermal time constants were 1.4 ± 0.4 s vs. 4.1 ± 0.5 s for the thermocouple and thermistor, respectively (Table 2).

Self-heating of the thermistor was comparable in both 434 MHz and 915 MHz EM fields. Whereas the thermocouple showed less self-heating than a thermistor in a 434 MHz EM field, but more self-heating compared to a thermistor in a 915 MHz EM field, 0.09 to 0.31 °C vs. 0.07 to 2.4 °C, respectively (Figure 9c, d).

Shaping the copper traces in horseshoe shaped meanders induced self-heating when the general direction of the traces were positioned perpendicular to the EM field, both in 434 MHz and 915 MHz EM fields (Figure 10). For 434 MHz, there seems to be a cut-off point between 85 and 105 mm where self-heating rapidly increases from an average of 0.2 °C to 1.56 °C. The thermal time constant of the thermistor was 3.3 ± 1.2 s vs. 3.3 ± 1.3 s for 434 MHz vs. 915 MHz respectively (Table 2).

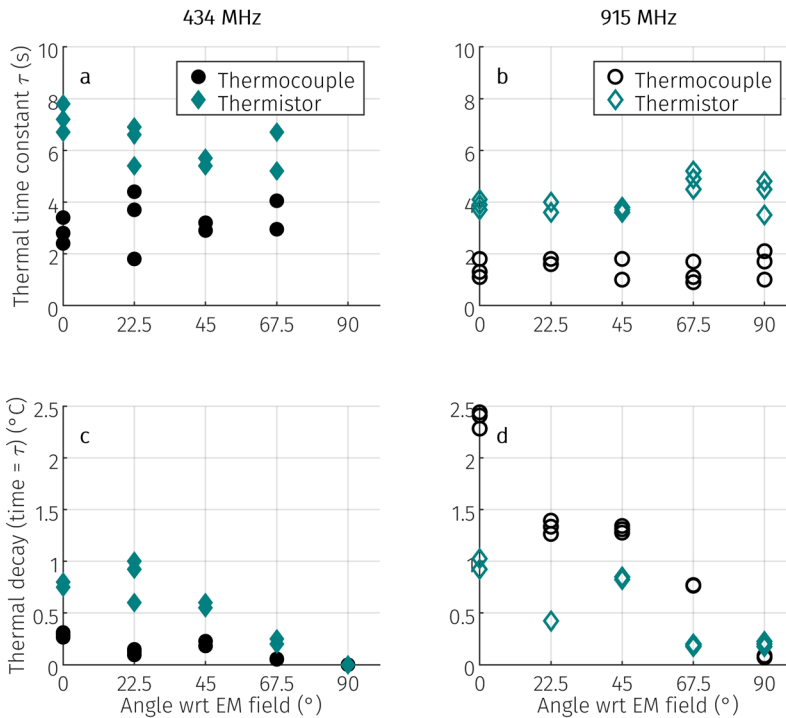


Figure 9. The measured response of a copper-constantan thermocouple probe (ELLA-CS, Hradec Králové, Czech Republic) and a 100 k Ω thermistor (NTCS0805E3104*MT, Vishay Intertechnology, Malvern, Pennsylvania) after three minutes of 50 W at 434 MHz and 915 MHz. The sensors were positioned between two water boluses circulating at 40 °C. The thermal time constant τ of the temperature decay after turning the power off (a, b) and the temperature decay at time = τ (c, d), i.e. self-heating, at 434 MHz (a, c) and 915 MHz (b, d).

Table 3. The amount of air due to the sheets with respect to the surface area of the water bolus in six patients with locoregional recurrent breast cancer.

| Sheet | Patient ID | Ratio largest air bubble/ water bolus surface (%) | Ratio air/ water bolus surface (%) |
|---------------------|------------|--|--|
| Thermocouple matrix | 1 | 0.2 | 4.1 |
| | 2 | 0.4 | 5.1 |
| | 3 | 0.2 | 4.5 |
| SPCB | 4 | 0.1 | 2.5 |
| | 5 | 0.9 | 3.5 |
| | 6 | 0.1 | 2.5 |

Abbreviations: SPCB= stretchable printed circuit board

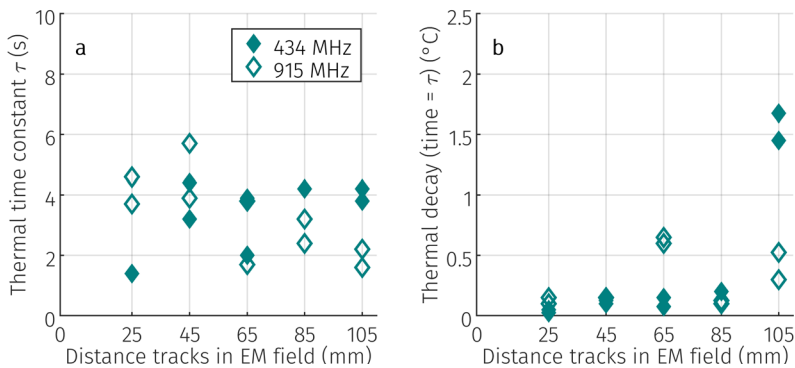


Figure 10. The horseshoe shape of the copper traces induced self-heating of the thermistor when positioned perpendicular to the main direction of a 434 MHz EM field. (a) The thermal time constant τ of the temperature decay, and (b) the temperature decay at time τ .

Table 2. The major requirements of the high-resolution thermal monitoring sheets for the skin surface during superficial microwave hyperthermia. The results of the thermocouple matrix and the SPCB were presented.

| | Required | Device tested | |
|------------------------------------|-------------------------------|--|---------------------------|
| | | Matrix | SPCB |
| Electrical circuit | | | |
| Spatial resolution | 40 x 40 mm [22] | 20 x 25 mm | 20 x 20 mm |
| Mean accuracy over 25 - 50 °C | ± 0.2 °C [17] | 0.06 ± 0.07 °C | 0.03 ± 0.02 °C |
| Maximum accuracy over 25 - 50 °C | ± 0.2 °C [17] | 0.18 °C | 0.05 °C |
| Temperature resolution | ≤ 0.1 °C [17] | 0.0156 °C | 0.0293 °C |
| Stability over 2 h | ≤ 0.1 °C h ⁻¹ [17] | < 0.01 °C h ⁻¹ | < 0.01 °C h ⁻¹ |
| Thermal conduction errors | ≤ 10 mm | 8.74 ± 2.18 mm (range 5.25 - 11.15 mm) | 2.15 mm |
| Supporting material | | | |
| Ability to follow patient contours | Yes | Yes | Yes |
| Air between skin and water bolus | < 5 % | 4.6 ± 0.5 % | 2.8 ± 0.6 % |
| Largest air bubble | < 1 % | 0.4 % | 0.9 % |

Table 2. Continued

| | <i>Required</i> | Device tested | |
|--|---------------------|----------------------|------------------------------|
| | | Matrix | SPCB |
| Electrical circuit in an EM field | | | |
| 434 MHz | | | |
| | | | <i>Straight copper leads</i> |
| 0 ° wrt EM field (–) | <i>Not required</i> | 0.29 ± 0.02 °C | 0.78 ± 0.03 °C |
| 90 ° wrt EM field (⊥) | < 0.1 °C | 0 °C | 0 °C |
| Thermal time constant | < 5 seconds | 3.2 ± 0.8 s | 6.4 ± 0.9 s |
| | | | <i>Horseshoe shaped</i> |
| 90 ° wrt EM field (⊥) 20 mm length | < 0.1 °C | | 0.05 °C |
| 90 ° wrt EM field (⊥) 105 mm length | < 0.1 °C | | 1.56 ± 0.16 °C |
| Thermal time constant | < 5 seconds | | 3.3 ± 1.2 s |
| 915 MHz | | | |
| | | | <i>Straight copper leads</i> |
| 0 ° wrt EM field (–) | <i>Not required</i> | 2.38 ± 0.08 °C | 0.99 ± 0.06 °C |
| 90 ° wrt EM field (⊥) | < 0.1 °C | 0.08 ± 0.01 °C | 0.20 ± 0.03 °C |
| Thermal time constant | < 5 seconds | 1.4 ± 0.4 s | 4.1 ± 0.5 s |
| | | | <i>Horseshoe shaped</i> |
| 90 ° wrt EM field (⊥) 20 mm length | < 0.1 °C | | 0.13 ± 0.04 °C |
| 90 ° wrt EM field (⊥) 105 mm length | < 0.1 °C | | 0.41 ± 0.16 °C |
| Thermal time constant | < 5 seconds | | 3.3 ± 1.3 s |

Abbreviations: SPCB= stretchable printed circuit board, EM= electromagnetic, wrt= with respect to.

Results were presented with mean ± SD when applicable. Results displayed in **bold** font were considered inadequate.

DISCUSSION

In this paper, two potential high-resolution thermal monitoring sheets were investigated to improve the spatial resolution for optimal temperature monitoring of the skin surface during hyperthermia treatments; the thermocouple matrix and the SPCB. The electrical circuit, supporting material and electromagnetic compatibility were investigated. The accuracy in the temperature range 25 - 50 °C was within 0.18 °C and 0.05 °C for the thermocouple and the thermistor, respectively. For both sheets, the temperature resolution was ≤ 0.03 °C, and the drift ≤ 0.01 °C h⁻¹ during two hours (Table 2). The accuracy of the thermocouple probe might be improved even further when the probe was calibrated in the clinically relevant temperature ranges, e.g. between 35 °C and 45 °C. Whereas the temperature resolution of the thermistor will improve by using a ADC with more bits or limiting the temperature range. Thermal conduction errors of the thermocouple probe ranged from 5.25 to 11.15 mm vs. 2.15 mm for the thermistor (Table 2). The thermal conduction error of the thermistor was equal to the length of the thermistor, thus there was no noticeable smearing across the copper leads of the thermistor. The thermal conduction errors for the thermocouple probe were higher compared to values from the literature for a five sensor copper-constantan thermocouple probe; varying from 4 - 7 mm [20] vs. 5.25 - 9.85 mm for the first five sensors of our thermocouple. A possible explanation for this small difference was that Dickinson [20] used thermocouple leads with different diameters: one \varnothing 50 μ m constantan and five \varnothing 60 μ m copper leads, while we used one \varnothing 70 μ m constantan and seven \varnothing 40 μ m copper leads. To reduce thermal conduction errors in a thermocouple probe, copper can be replaced by manganin which has a 17 times lower thermal conductivity than copper [20, 29]. This was done by Dickinson [20] who reported much smaller conduction errors for five sensor manganin-constantan thermocouple probes; 1.9 - 2.7 mm.

The supporting materials could excellently follow body contours, where an acceptable amount of air (≤ 5.1 %) was present between the water bolus and the skin due to the matrix and SPCB (Table 2). The amount of air will likely be even lower in the clinical situation where the water bolus of the applicator is firmly kept in position by the hyperthermia devices (ALBA ON 4000, Medlogix, Italy; BSD-500, Pyrexar, Salt Lake City, UT, USA) or Velcro tape.

The perturbation of temperature readings due to microwave interference in electronic circuits was quantified in both 434 and 915 MHz EM fields. Since the sampling frequency was only 0.5 - 1 Hz, the measurement of self-heating and the thermal time constant might be underestimated since the exact temperature at the moment when power was switched off was likely not measured. When the straight leads were positioned perpendicular (90 °)

to the main direction of the EM field there was no perturbation noticeable. However, when the leads were positioned not perpendicular, self-heating of the sensors occurred. The thermistor showed higher thermal time constants than the thermocouple (Table 2), likely due to the larger size of the thermistor and thus more heat capacity. The thermocouple had approximately two-fold higher self-heating at 915 MHz than at 434 MHz, while self-heating of the thermistor was similar (Figure 9). An explanation for this phenomenon could be that the wavelength at 915 MHz was shorter than 434 MHz, which could potentially increase the risk on perturbation of the electrical circuit. It has been advised, to prevent perturbation of temperature readings by metal sensors in an EM field during hyperthermia, to take the temperature readings after five seconds of power off [18].

The horseshoe shape of the copper traces was responsible for inducing in rare cases potentially hazardous self-heating of the thermistors when an EM field was applied (Figure 10). A possible explanation was that due to the horseshoe shape numerous small sections of the copper trace were aligned in the direction of the EM field, allowing microwave interference of the electrical circuit. However, the exact reason why this occurred requires further in-depth investigation. A logical solution to reduce this self-heating is by using high resistance conductive material for the horseshoe shape tracks as with Bowman probes [19]. At the moment, carbon, tin indium oxide or other materials with a high conductivity, cannot be used in the present etching techniques that are used to produce SPCBs. However, advances in the SPCB field go rapidly and using carbon as the conductive material remains a viable option in this field of investigation.

The results of our experiments were obtained with good thermal contact of the sensors to the water bolus. Higher self-heating values might occur when more air is present between the water bolus and the patient. Further research should be performed to investigate the self-heating and time constant in the case of less ideal thermal contact. However, in clinical practice the pressure exerted by the weight of the applicator plus water bolus will probably ensure that the water bolus normally deforms to follow the contour of the skin and sheet, ensuring good thermal contact, certainly at the location of the temperature sensors where the sheet is slightly thicker resulting in the sensors being pressed even more vigorously into the skin. Suboptimal contact is thus only likely to occur for skin surfaces with large irregularities, which rarely occur. Unexpectedly high temperatures during treatment could indicate self-heating of the sensors. Whether self-heating occurs can be checked by turning the power off and monitoring the temperature change in the next seconds. A steep temperature decay indicates self-heating of the sensors. In that case, the position of these sensors should be adjusted, such that the probes are aligned perpendicular to the EM-field.

Implementing a standard method to measure skin surface temperature with a high spatial resolution can decrease thermal toxicity and improve hyperthermia treatment quality. It should be noted that even with a high spatial resolution of superficial measurements, invasive thermometry remains necessary. After all, only the invasively measured thermal dose has been demonstrated to have a relationship with treatment response, local control and overall survival [1–10]. Having insufficient invasive temperature data for optimized power control is a problem that will not be resolved until breakthroughs in hardware and/or modelling make three-dimensional, non-invasive high-resolution thermometry possible [35]. Although temperature simulations might increase insight, they are associated with uncertainties in perfusion and dielectric tissue properties, resulting in inaccurate predictions of the achieved temperatures [36, 37].

On condition that the sensors should be positioned perpendicular to the main direction of the EM field, the thermocouple matrix was at this moment closest to clinical application. The thermocouple matrix had 56 sensors with a resolution of one sensor every five cm². Higher spatial resolution was not possible, unless the probes were positioned closer together and multiple thermometry systems were combined (standard 64 channel thermometry system). The SPCB on the other hand had much potential to increase spatial resolution even further, and its design was more flexible and could be individualized per patient although this was time consuming. Since scar tissue was more important for temperature monitoring [11], the design could be individualized to include more sensors in that particular area. Whereas the thermocouple matrix does not allow this kind of flexibility, it does allow for an additional multisensor thermocouple probe for invasive temperature measurements. Furthermore, placing the sheets on the skin surface was likely easier and quicker, compared to previously developed methods. The sensors incorporated on the sheets are probably more durable than individual sensors or probes. The costs for a reusable SPCB is approximately 1500 euros, whereas the reusable thermocouple matrix will be included with the ALBA ON 4000 and individual seven sensor thermocouple probes cost approximately 250 euros each. This combination of acceptable cost, flexibility and ease of use, makes that these sheets have a strong potential for general clinical implementation in hyperthermia centers.

Compared to clinically used thermometry systems with a high spatial resolution [21, 23–25], both sheets were either less fragile, less time-consuming to position or had a higher spatial resolution. The high resolution methods used in Rotterdam [23] and Amsterdam [24] employ individual multisensory probes that were time-consuming to position. The thermal monitoring sheet [21, 25] developed at Duke in 2008 did allow rapid and reproducible positioning, but it comprises only 16 sensors and has never been taken into production. The copper-constantan thermocouple probes used in Amsterdam were identical to the copper constantan thermocouple probes described in this paper. Fiber-optic probes used

in the other solutions [21, 23, 25] were fragile and expensive but very accurate. Whereas thermal mapping was limited in temporal monitoring since the time required for a single map varied from two to nine minutes [38, 39].

Before clinical application of either of the two sheets, thorough investigations are required on the influence of an additional layer of material between the patient and the water bolus of the superficial hyperthermia applicator [21, 25]. The magnitude and shape of the EM field inside the patient could be influenced by adding an additional sheet with a high density of metal wires between the water bolus and the patient [21]. Additional SAR measurements are required to evaluate the effect of the sheets on the SAR distribution. Furthermore, the water bolus of a superficial hyperthermia device has, besides coupling of the electromagnetic energy to the patient, the important function to reduce hot- and cold spots on the skin [17]. Adding an extra layer of material could reduce the heat transfer of the water bolus to the skin [40]. It is important to investigate to which extent the sheets affect both the coupling and cooling ability of the water bolus before clinical applications of a new thermal monitoring sheet.

CONCLUSION

Two possible thermal monitoring sheets to improve the spatial resolution of skin surface temperature monitoring during superficial hyperthermia were investigated. The thermocouple matrix (Medlogix, Italy, Rome) was accurate, EM compatible, and could follow the body contours. The stretchable printed circuit board sheet was accurate and flexible, but requires further in-depth investigation to analyze the occasional perturbation of temperature readings due to the EM field. Both sheets show potential, where the thermocouple matrix was the most promising for clinical application.

REFERENCES

- [1] Bakker A, van der Zee J, van Tienhoven G, et al. Temperature and thermal dose during radiotherapy and hyperthermia for recurrent breast cancer are related to clinical outcome and thermal toxicity: A systematic review. *Int J Hyperth* 2019; 36: 1024–1039.
- [2] Franckena M, Fatehi D, Bruijine M de, et al. Hyperthermia dose-effect relationship in 420 patients with cervical cancer treated with combined radiotherapy and hyperthermia. *Eur J Cancer* 2009; 45: 1969–1978.
- [3] Kroesen M, Mulder HT, van Holthe JML, et al. Confirmation of thermal dose as a predictor of local control in cervical carcinoma patients treated with state-of-the-art radiation therapy and hyperthermia. *Radiother Oncol* 2019; 140: 150–158.
- [4] Overgaard J, Gonzalez Gonzalez D, Hulshof MC, et al. Hyperthermia as an adjuvant to radiation therapy of recurrent or metastatic malignant melanoma. A multicentre randomized trial by the European Society for Hyperthermic Oncology. *Int J Hyperth* 1996; 12: 3–20.
- [5] Oleson JR, Samulski TV, Leopold KA, et al. Sensitivity of hyperthermia trial outcomes to temperature and time: Implications for thermal goals of treatment. *Int J Radiat Oncol Biol Phys* 1993; 25: 289–297.
- [6] Issels RD, Mittermüller J, Gerl A, et al. Improvement of local control by regional hyperthermia combined with systemic chemotherapy (ifosfamide plus etoposide) in advanced sarcomas: Updated report on 65 patients. *J Cancer Res Clin Oncol* 1991; 117: 141–147.
- [7] Wust P, Rau B, Gellermann J, et al. Radiochemotherapy and hyperthermia in the treatment of rectal cancer. *Recent Results Cancer Res* 1998; 146: 175–191.
- [8] Sneed PK, Stauffer PR, Gutin PH, et al. Interstitial irradiation and hyperthermia for the treatment of recurrent malignant brain tumors. *Neurosurgery* 1991; 28: 206–215.
- [9] Emami B, Perez CA, Konefal J, et al. Thermoradiotherapy of malignant melanoma. *Int J Hyperth* 1988; 4: 373–381.
- [10] Jones EL, Oleson JR, Prosnitz LR, et al. Randomized trial of hyperthermia and radiation for superficial tumors. *J Clin Oncol* 2005; 23: 3079–3085.
- [11] Bakker A, Kolff MW, Holman R, et al. Thermal skin damage during reirradiation and hyperthermia is time-temperature dependent. *Int J Radiat Oncol Biol Phys* 2017; 98: 392–399.
- [12] Kapp DS, Cox RS, Fessenden P, et al. Parameters predictive for complications of treatment with combined hyperthermia and radiation therapy. *Int J Radiat Oncol Biol Phys* 1992; 22: 999–1008.
- [13] Linthorst M, Baaijens M, Wiggendaad R, et al. Local control rate after the combination of re-irradiation and hyperthermia for irresectable recurrent breast cancer: Results in 248 patients. *Radiother Oncol* 2015; 117: 217–222.
- [14] Linthorst M, van Geel AN, Baaijens M, et al. Re-irradiation and hyperthermia after surgery for recurrent breast cancer. *Radiother Oncol* 2013; 109: 188–193.
- [15] Oldenburg S, Griesdoorn V, Van Os R, et al. Reirradiation and hyperthermia for irresectable locoregional recurrent breast cancer in previously irradiated area: Size matters. *Radiother Oncol* 2015; 117: 223–228.
- [16] Oldenburg S, van Os RM, van Rij CM, et al. Elective re-irradiation and hyperthermia following resection of persistent locoregional recurrent breast cancer: A retrospective study. *Int J Hyperth* 2010; 26: 136–144.

- [17] Dobšiček Trefná H, Crezee J, Schmidt M, et al. Quality assurance guidelines for superficial hyperthermia clinical trials: I. Clinical requirements. *Int J Hyperth* 2017; 33: 471–482.
- [18] Shrivastava P, Saylor TK, Matloubieh AY, et al. Hyperthermia thermometry evaluation: criteria and guidelines. *Int J Radiat Oncol Biol Phys* 1988; 14: 327–335.
- [19] Bowman RR. A probe for measuring temperature in radio-frequency-heated material. *IEEE Trans Microw Theory Tech* 1976; 43–45.
- [20] Dickinson RJ. Thermal conduction errors of manganin-constantan thermocouple arrays. *Phys Med Biol* 1985; 30: 445–453.
- [21] Arunachalam K, Maccarini PF, Juang T, et al. Performance evaluation of a conformal thermal monitoring sheet sensor array for measurement of surface temperature distributions during superficial hyperthermia treatments. *Int J Hyperth* 2008; 24: 313–325.
- [22] Bakker A, Holman R, Rodrigues DB, et al. Analysis of the required number of sensors for adequate monitoring of skin temperature distribution during superficial microwave hyperthermia treatment. *Int J Hyperth* 2018; 34: 910–917.
- [23] van Rhooon G. Personal communications.
- [24] de Leeuw AAC, Crezee J, Lagendijk JJW. Temperature and SAR measurements in deep-body hyperthermia with thermocouple thermometry. *Int J Hyperth* 1993; 9: 685–697.
- [25] Arunachalam K, Maccarini PF, Stauffer PR. A thermal monitoring sheet with low influence from adjacent waterbolus for tissue surface thermometry during clinical hyperthermia. *IEEE Trans Biomed Eng* 2008; 55: 2397–2406.
- [26] Ostmann A, Loher T, Seckell M, et al. Manufacturing concepts for stretchable electronic systems. *2008 3rd Int Microsystems, Packag Assem Circuits Technol Conf IMPACT 2008* 2008; 24–27.
- [27] Finline QPI BV. Stretchable printed circuit boards, <http://qipigroup.nl/producten-en-services/pcb-technologieen/rekbare-printplaat-technologie> (2019, accessed 10 October 2019).
- [28] Vishay BCcomponents. SMD 0805 , Glass Protected NTC Thermistors. *08-08-2012* 2012; 1–8.
- [29] van der Kooij JF, Crezee J, Lagendijk JJW. Thermal properties of capacitively coupled electrodes in interstitial hyperthermia. *Phys Med Biol* 1998; 43: 139–151.
- [30] Kok HP, De Greef M, Correia D, et al. FDTD simulations to assess the performance of CFMA-434 applicators for superficial hyperthermia. *Int J Hyperth* 2009; 25: 462–476.
- [31] Gabriele P, Ferrara T, Baiotto B, et al. Radio hyperthermia for re-treatment of superficial tumours. *Int J Hyperth* 2009; 25: 189–198.
- [32] Sherar M, Liu F, Newcombe D, et al. Beam shaping for microwave hyperthermia applicators. *Int J Radiat Oncol Biol Phys* 1993; 25: 849–857.
- [33] Stauffer PR, Rodrigues DB, Sinahon R, et al. Using a conformal water bolus to adjust heating patterns of microwave waveguide applicators. In: Ryan T (ed) *Energy-based Treatment of Tissue and Assessment IX*. 2017, p. 100660N.
- [34] Rodrigues DB, Hurwitz MD, Maccarini PF, et al. Optimization of chest wall hyperthermia treatment using a virtual human chest model. In: *European Conference on Antennas and Propagation*. 2015.
- [35] Lee ER, Kapp DS, Lohrbach A, et al. Influence of water bolus temperature on measured skin surface and intradermal temperatures. *Int J Hyperth* 1994; 10: 59–72.
- [36] Gabriel C, Gabriel S, Corthout E. The dielectric properties of biological tissues: I. Literature survey. *Phys Med Biol* 1996; 41: 2231–2249.
- [37] Balidemaj E, de Boer P, van Lier ALHMW, et al. In vivo electric conductivity of cervical cancer patients based on B1+ maps at 3T MRI. *Phys Med Biol* 2016; 61: 1596–1607.
- [38] Gibbs FA. ‘Thermal mapping’ in experimental cancer treatment with hyperthermia: Description and use of a semi-automatic system. *Int J Radiat Oncol Biol Phys* 1983; 9: 1057–1063.

- [39] Ryan TP, Wikoff RP, Hoopests PJ. Design of an automated temperature mapping system for ultrasound or microwave hyperthermia. *J Biomech Eng* 1991; 13: 348–354.
- [40] Legendijk JJW. Heat transfer in tissues. In: Field SB, Franconi C (eds) *Physics and Technology of Hyperthermia*. Dordrecht: Springer, 1987, pp. 517–552.